Acta Geotechnica (2021) 16:1043–1052
https://doi.org/10.1007/s11440-020-01080-x

RESEARCH PAPER

Effects of particle shape on the cushioning mechanics of rock-filled gabions

Yuchen Su[1] · Clarence E. Choi[2]

Received: 23 February 2020 / Accepted: 12 September 2020 / Published online: 25 September 2020

Abstract
Rock-filled gabions are commonly installed in front of reinforced concrete structures to reduce concentrated impact loads induced by rock fall and boulders entrained in debris flows. The cushioning performance of rock-filled gabions may vary depending on the shape of rock fragments used. In this paper, a parametric study was carried out using the discrete element method to discern the effects of particle shape on the cushioning performance of rock-filled gabion against dynamic boulder impact. Four particle sphericities were adopted to model angular, sub-angular, sub-rounded and rounded particles. DEM simulations reveal that the boulder penetration depth decreases with particle angularity. Thus, a thicker cushioning layer should be used in design if particles are rounded. More importantly, the impact and transmitted forces on a reinforced concrete barrier increased with particle angularity. This is because angular assemblies have more contact points, which enable more stable force chains that can sustain higher loads. The load diffusion angle for rounded particles is up to 20° larger compared to angular particles, suggesting that as particle angularity governs the load spreading ability of a cushioning layer. In general, rocks with rounded morphology should be adopted where possible to reduce transmitted loads and distribute loads more uniformly.

Keywords Debris flow · Discrete element method · Particle shape · Rigid barrier · Rock-filled gabion · Rock fall

1 Introduction

Debris flow consists of a mixture of poorly sorted sediments, ranging in size from clay to boulder [13, 40]. The mechanism of particle size segregation enables large boulders to migrate to the front of a flow [41]. These boulders can then induce highly concentrated loads, which may cause significant damage to infrastructure [5, 11, 44, 45, 55, 59]. To arrest these boulders, reinforced concrete barriers are commonly constructed along the predicted flow paths [6, 18, 19, 24, 28, 30, 31, 34]. In front of these barriers, a layer of rock-filled gabion is commonly installed for additional protection.

To study the performance of cushioning layers, large-scale boulder impact tests are commonly used [20–23]. Ng et al. [29] modelled up to six successive boulder impacts at an energy level of 70 kJ on a rock-filled gabion cushioning layer in front of a reinforced concrete barrier. They reported that by adopting rock-filled gabion cushioning layer, the design impact load can be reduced by a factor of two. The load reduction is mainly attributed to the collapse and formation of force chains among rock fragments inside a gabion cell as it is impacted.

Natural rock fragments used for cushioning generally have irregular shapes (Fig. 1). The shape governs the degree to which fragments interlock and therefore influences the shear resistance of the entire assembly. Experiments are commonly used to investigate the effects of particle shape [2, 54]. Yang and Wei [52] conducted a series of laboratory tests to explore the role of particle shape on the shear behaviour of mixture of sand and fines. Experiments showed that the critical state friction angle increases with the percentage of angular particles. Also, force chains in granular materials with grains that are more

✉ Clarence E. Choi
cechoi@hku.hk

[1] College of Mechanics and Materials, Hohai University, Nanjing 210098, China

[2] Department of Civil Engineering, The University of Hong Kong, Pokfulam, Hong Kong SAR, China

Fig. 1 Front view of rock-filled gabion cushion layer

rounded were more susceptible to collapse. Yang and Luo [53] also reported that the shearing behaviour of granular material is significantly influenced by particle shape. Their experiments showed that the angular grains are less susceptible to liquefaction. Xiao et al. [49] reported that the peak-state deviatoric stress, peak-state axial strain and peak-state friction angle decreased with particle angularity. Xiao et al. [50] further revealed that the unconfined compressive strength decreases with the particle angularity. Evidently, particle shape significantly influences the mechanical response of granular materials.

The discrete element method is another approach that is commonly used to shed light on the mechanical response of granular materials [4]. Muthuswamy and Tordesillas [27] and Tordesillas et al. [39] carried out a series of discrete element simulations to investigate the effects of contact friction and bulk density on the behaviour of force chains inside a granular assembly. Their findings showed that straighter force chains with higher contact friction can sustain higher loads. Also, granular assemblies become stiffer as the load bearing capacity of the force chains increases. Zhang et al. [57] and Su et al. [35] reported that force chains made of smaller particles may collapse more easily. However, assemblies with smaller particles have more contact points, which are more effective at spreading load.

A multitude of studies [7–9, 25, 42, 43, 56, 58] have reported that idealising an assembly of angular particles as spheres will give an incorrect mechanical response. The effects of particle shape on the mechanical response of granular materials were also reported by other researchers [2, 16, 32, 33, 48]. In these studies, it was concluded that the friction angle generally increases with particle angularity. A method commonly used to simulate particle angularity using spherical discrete elements is by applying rolling resistance to capture the effects of particle eccentricity [47]. However, irregular shapes should allow particle rotation as well as resisting it, while prescribed rolling friction only provides rotational resistance. Furthermore, the repose angle for an assembly of irregular shapes differs compared to an assembly of spheres with rotational resistance [37]. In another numerical approach, Xu et al. [51] adopted a clump composed of several subparticles with unbroken bonds to model the effects of particle shape, which proved to be one of the most ideal approaches to model the effects of particle shape.

In this paper, the effects of particle shape on the cushioning mechanism of granular materials are investigated by carrying out a parametric study using the DEM. The influences of particle shape on the attenuation of the boulder impact force and the reduction in the transmitted loads are examined. Findings will be used to provide a basis to optimise the design and performance of rock-filled gabion cushioning layers in the field.

2 Methodology

In this study, a commercial software called Particle Flow Code PFC^{3D} was used to investigate the mechanical response of rock-filled gabions subjected to boulder impact. The contact mechanics between particles is governed by the Hertz contact model, which is a nonlinear formulation based on the theory of Mindlin [26]. For each time step, the normal contact force is the product of the incremental overlap and the normal contact stiffness for each particle. The equations used to determine the normal and shear contact forces are given as follows [14]:

$$\mathrm{d}F_n = \frac{3}{2}K_n(u_n)^{0.5}\mathrm{d}u_n \tag{1}$$

The shear contact force for each particle is the product of the incremental overlap and the shear contact stiffness. The shear contact force is governed by Coulomb's law of friction. The equations used to determine the incremental normal and shear contact forces are given as follows [14]:

$$dF_t = K_t du_t \xi(F_n \tan\phi - F_t) \quad (2)$$

where ϕ is the internal friction angle and ξ is the Heaviside function where $\xi(x) = 1$ when $x > 0$ and $\xi(x) = 0$ when $x \leq 0$, K_n and K_t are the normal and shear contact stiffnesses, which are calculated using the following equations:

$$K_n = \frac{2\sqrt{2R_e}G}{3(1-v)} \quad (3)$$

$$K_t = 2\frac{(3G^2(1-v)R_e)^{1/3}}{2-v}F_n^{1/3} \quad (4)$$

where R_e is the effective radius, G is the shear modulus and υ is the Poisson's ratio of a grain.

2.1 Shape factor

Shape factors such as sphericity, roundness and roughness are widely adopted to describe the particle shape [46]. Roundness (R) was proposed to determine the sharpness of the edge of a particle [60]. Roundness is expressed as:

$$R = \frac{\sum \frac{r}{r'}}{N} \quad (5)$$

where r is the radius of curvature of a corner of the particle surface, r' is the radius of maximum inscribed circle in the projected plane and N is the number of corners. A roundness value (R) greater than 0.6 indicates high roundness and R less than 0.4 represents low roundness. Surface roughness (S) is given as the ratio of perimeter of the particle to the enclosed perimeter [15, 16, 46], which is defined as the perimeter that goes from tip to tip of a particle. A sphere has a roughness of 1.0.

In this study, particle sphericity is considered as a key parameter, which is defined as the ratio of maximum radius of the largest inscribed sphere (R_{max}) to the radius of the smallest circumscribed sphere (R_{min}) [48]. Sphericity represents the similarity between particle length, width and height. Sphericity increases as the shape of a particle more closely resembles that of a sphere. A sphericity of unity means the particle is perfectly spherical. By contrast, a sphericity close to zero means the shape of the particle is needle-like.

2.2 Field test set-up of Ng et al. [29]

Large-scale pendulum impact test results reported by Ng et al. [29] on the dynamic response of rock-filled gabions are used to compare with the computed results in this study. Figure 2 shows a schematic side view of field test set-up, which consists of a concrete boulder, a steel frame and rock-filled gabions in front of a rigid reinforced concrete barrier. The concrete boulder has a mass of 2000 kg and is suspended by two steel strand cables. A mechanical latch is installed to release the concrete boulder. A steel frame with a height of 6 m is constructed to suspend the concrete boulder, which swings and impacts the rock-filled gabion cushioning layer. The cushioning layer is constructed using nine separate cubic gabion baskets with a nominal length of 1 m. The size of the rock fragments ranges from 160 to 300 mm in diameter [10].

2.3 Discrete element modelling

The main purpose of numerical model is to understand the dynamic interaction between a model boulder and rock fragments inside the gabion basket. Therefore, to simplify the model and reduce computational time, the steel frame, steel strand cables used to suspend the concrete boulder and gabion baskets used to contain baskets were not explicitly modelled. Figure 3 shows an oblique view of the numerical model, which includes a spherical boulder and a cell to retain the rock fragments. For each simulation, a sphere with a mass of 2000 kg is given an initial velocity of 8.4 m/s to simulate an impact energy of 70 kJ [29]. A box with a length, height and width of 3 m, 3 m and 1 m, respectively, was used to simulate the rock-filled gabion layer. A total of 776 discrete elements were generated in the box with a target initial porosity of 0.4 and allowed to settle under the influence of gravity. The particle sizes selected, 160 mm to 300 mm, were based on design guidelines [10]. A friction angle of 30° was adopted [3,30].

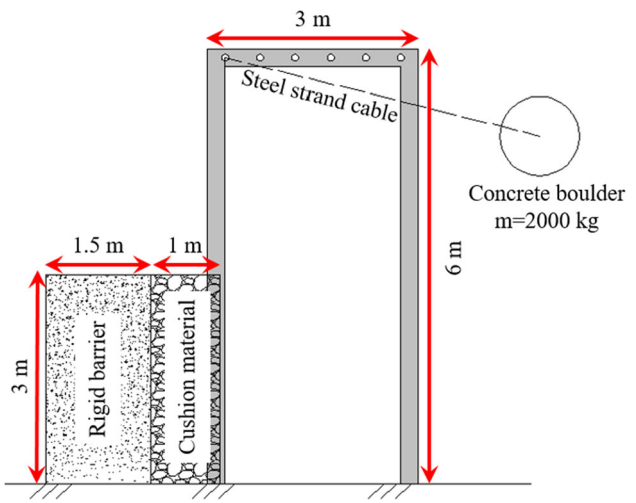

Fig. 2 Schematic view of pendulum impact test set-up reported in Ng et al. [29]

Table 1 DEM model parameters used in the current study

Parameters	Values
Density (kg/m^3)	2650
Shear modulus (MPa)	4×10^6
Poisson's ratio	0.25
Local friction angle (°)	30
Porosity	0.4

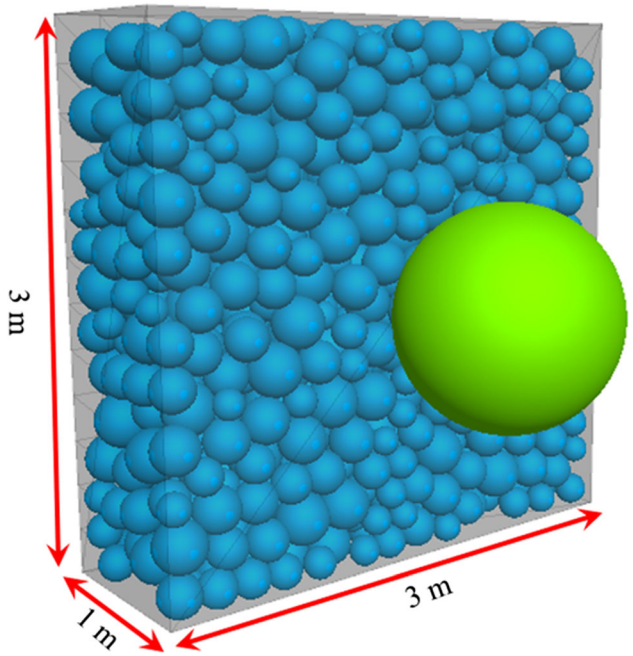

Fig. 3 Oblique view of DEM model

The adopted parameters used to describe rock fragments are summarized in Table 1. To monitor the horizontal and vertical load distributions on a rigid barrier, eight measurement regions (2250 m^2 each), coinciding with the load cells used in the field tests [29], were defined on the backside wall (Fig. 4).

To model the effects of particle shape on the impact dynamics, the clump option was used. A clump is a rigid body comprised of a series rigid spheres bonded together. The calculation of contacts between each sphere in a clump is ignored in each computational cycle. In this study, a total of 776 spherical particles were generated, and then, the particles were replaced with clumps with same volume. It was reported by Shin and Santamatina [32] that the measured sphericities for natural and crushed sand range from 0.5 to 0.9. To compare various particle sphericities, four clumps with particle sphericities of 0.5, 0.6, 0.8 and 1.0 were investigated. A summary of the simulation plan is given in Table 2.

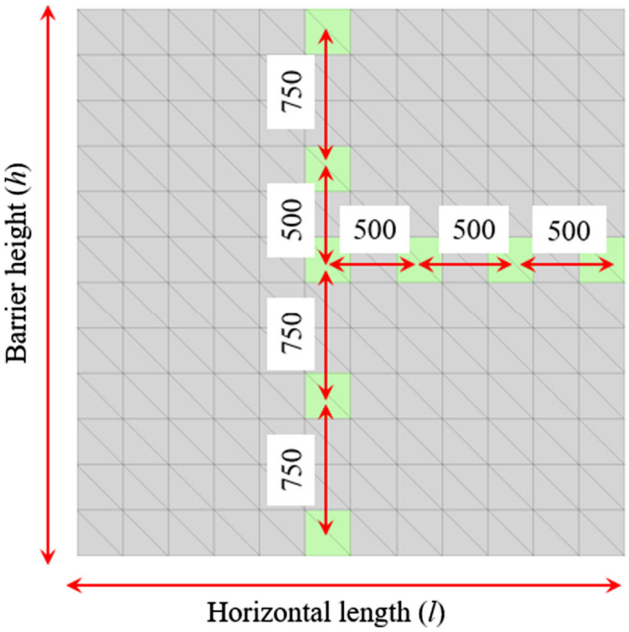

Fig. 4 Eight points of measurements for the computed transmitted load distributions on the rigid barrier (all dimensions in mm)

Table 2 Summary of numerical simulation plans

Test ID	Particle sphericity (R_{imax}/R_{cmin})	Clump
Rounded (R)	1.0	
Sub-rounded (SR)	0.8	
Sub-angular (SA)	0.6	
Angular (A)	0.5	

2.4 Comparison of boulder impact force

Figure 5 shows a comparison between the measured and computed boulder impact forces. The shear modulus used to describe the rocks is calibrated to match the maximum boulder impact force. The difference between the measured and computed maximum boulder impact force is less than 5%, indicating that the input parameters adopted are suitable for predicting the maximum boulder impact force for assemblies with different shapes. Furthermore, large fluctuations were observed in both the measured and computed

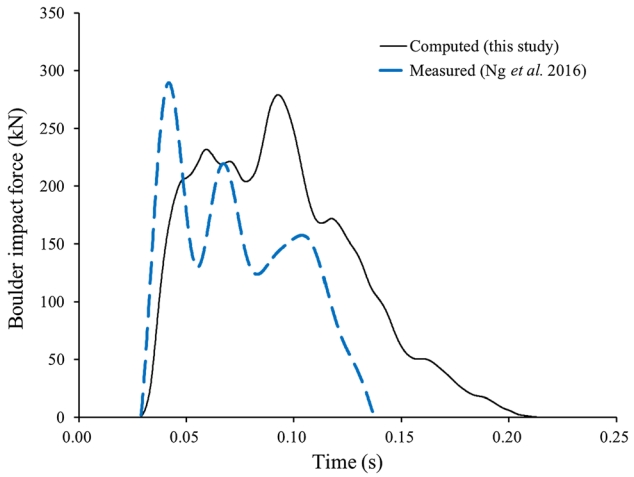

Fig. 5 Comparison of boulder impact forces between computed and measured results

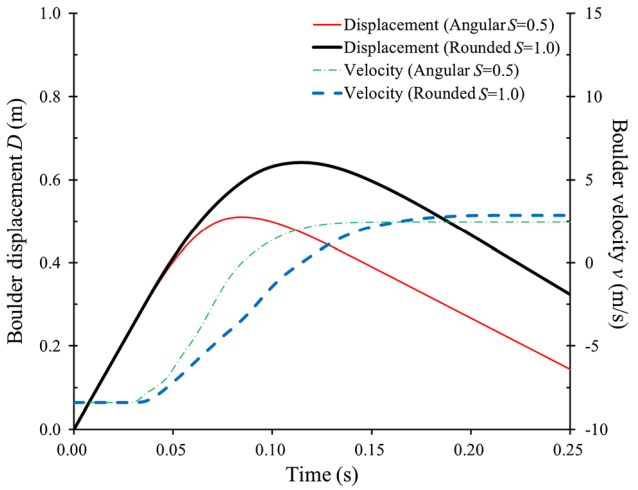

Fig. 6 Comparison of boulder displacement and velocity between angular and rounded particles

results. These fluctuations are caused by the collapse of force chains during impact.

The area under the impact force curve represents the momentum. The computed momentum is about 30% larger compared to the measured momentum. One possible feature that may contribute to differences between the computed and measured momentum is particle crushing. In the field tests, crushing was observed after each test. However, crushing is not captured in the idealised numerical simulations to study the fundamental grain-scale effects of particle shape. Without the effect of crushing, less energy is absorbed by the granular assembly and more energy is reflected back to the boulder, thereby increasing the rebound velocity of the boulder.

2.5 Effects of particle shape

2.5.1 Time histories of boulder penetration depth and velocity

A parametric study was carried out to investigate the effects of particle shape on the cushioning mechanisms of rock-filled gabions. Figure 6 shows the computed time histories of boulder displacement (D) and boulder velocity (v) for angular (S = 0.5) and rounded particles (S = 1.0). The initial distance between boulder and particle assembly is 0.24 m. Therefore, the boulder has a displacement of 0.24 m with velocity of 8.4 m/s and impact occurs at 0.03 s. By subtracting the initial displacement, the maximum calculated boulder penetration depths are 0.27 m and 0.40 m for the angular and rounded particles, respectively. The maximum boulder penetration depth for rounded particles is 1.5 times larger compared to that of angular particles. For the same impact energy, a larger penetration depth requires more particle movement. Shin and Santamatina [32] reported that angularity restricts particle movement, thereby increasing the shear resistance of a granular assembly. According to international design guidelines for rock-filled gabions [1], the recommended cushioning layer thickness should be at least the two times the maximum penetration depth. Based on the parametric study on shape effects, the cushioning layer thickness for rounded particles should be designed to be larger compared to that for angular particles. A thickness of 1 m is appropriate for both the rounded and angular particles simulated in this study.

2.5.2 Maximum boulder impact force

Figure 7 shows a comparison of the computed time histories of the boulder impact force among the four particle shapes simulated, specifically angular, sub-angular, sub-

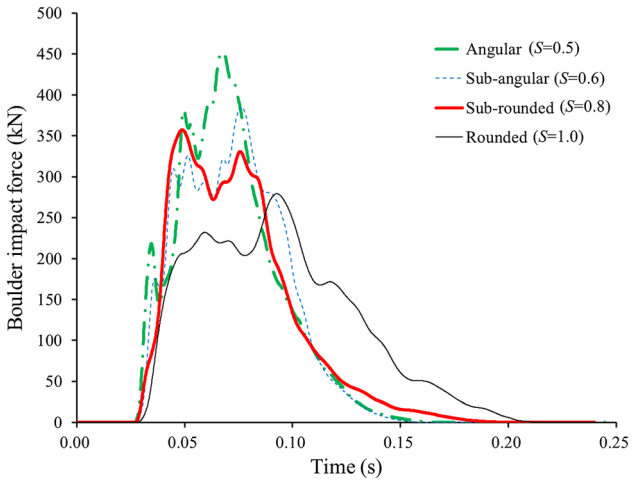

Fig. 7 Comparison of boulder impact force with different particle shapes

rounded and rounded. This maximum boulder impact force increases with particle angularity. The maximum boulder impact force of 451 kN for angular particles is about 1.6 times larger compared to that of rounded particles. This means that the maximum boulder impact force increases with particle angularity. This is because angularity restricts particle rotations during impact, which enables force chains to sustain higher loads. Likewise, Althhafi et al. [2] reported that by increasing particle angularity, grain rotations are restricted, which give rise to stiffer granular assemblies. Hadda and Wan [12] also reported that the granular fabric progressively changes from an anisotropic to an isotropic state under cyclic loading. More specifically, the contact numbers and densities change with successive impact. These finding corroborate the importance of capturing grain-scale fabric, particularly particle shape, for modelling the dynamic response of rock-filled gabion cushioning material.

Figure 8a, b shows side views of the force chain distributions when the maximum impact force occurs for angular and rounded particles, respectively. The thickness of the force chains is scaled to enhance visualisation. The force chains at the bottom of cushioning layer, under higher confining stress, are denser and thicker compared to those at the top because of the influence of gravity. Similarly, Ng et al. [29] and Su et al. [36] also reported that higher loads are transmitted downwards due to the overburden provided by the overlying gabion cells. Furthermore, the load diffusion angles, which provide an indication of the load spreading capability of a cushioning layer, are 30° and 50° for angular and rounded particles, respectively. Evidently, the effects of particle shape strongly influence the load diffusion angle, which decreases with particle angularity.

Figure 9 shows the average contact force carried by the force chains when the cushioning layer is impacted. The maximum average contact force for angular particles is about 1.8 times larger compared to that for rounded particles, corroborating that higher loads can be supported by angular particles. Furthermore, the loading and unloading slopes for angular particles are much steeper compared to those of rounded particles, suggesting that angularity affects stiffness.

The maximum number of force chains for rounded particles is about 1.4 times larger compared to that of angular particles. This means more force chains are required to resist the boulder impact force with rounded particles compared to angular particles. Evidently, force chains composed of angular particles are more stable compared to that of rounded particles.

Figure 10 shows a comparison of the average coordination number (Z) between angular and rounded particles.

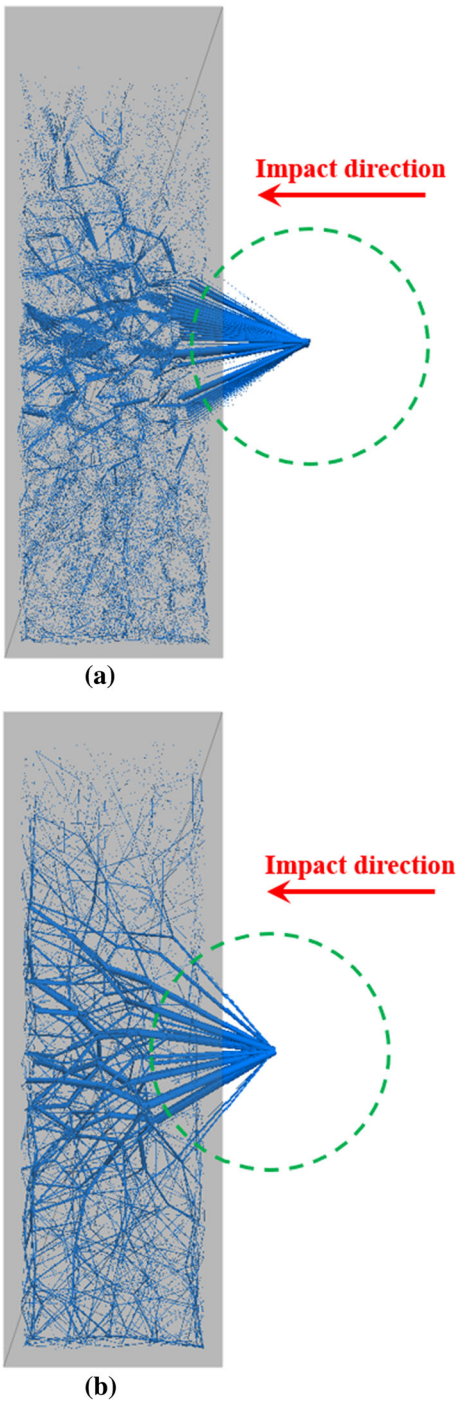

Fig. 8 Side views of force chain distributions at the moment of maximum boulder impact force: **a** angular particles (S = 0.5); **b** rounded particles (S = 1.0)

The average coordination number is calculated as follows [38]:

$$Z = \frac{2C - N_1}{N - N_0 - N_1} \tag{6}$$

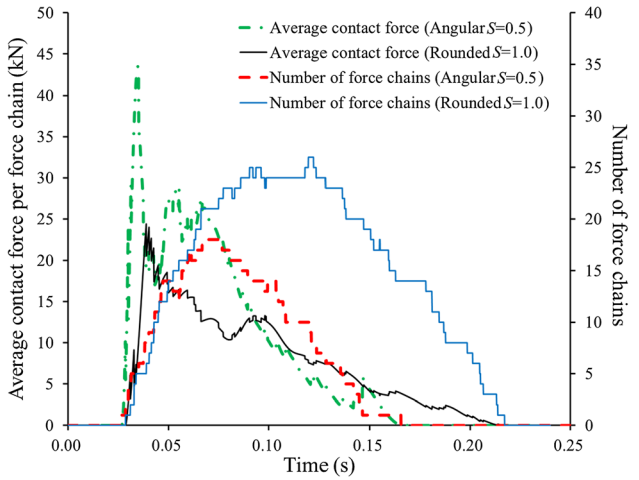

Fig. 9 Comparison of the average contact force and number of force chains between angular particles (S = 0.50) and rounded particles (S = 1.0)

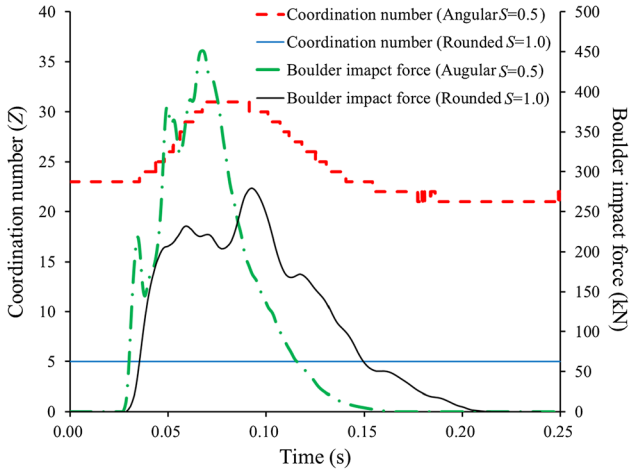

Fig. 10 Comparison of average coordination number Z and boulder impact force between angular particles (S = 0.50) and rounded particles (S = 1.0)

where C is the number of contacts among particles, N is the number of particles, and N_0 and N_1 represent the number of particles with no contacts and one contact, respectively. The average coordination number provides the average number of contacts that contribute to the mechanical stability of a granular assembly.

The rounded particles exhibit a relatively constant average coordination number of five during the impact process. However, the average coordination number for angular particles reaches a maximum of 31, which is six times larger compared to that of the rounded particles. The maximum coordination number for angular particles is about six times larger compared to that of rounded particles. Similar observations were reported by Wang and Song [48], indicating that more contacts are formed for particles with increasing angularity. More contacts in an assembly enable higher sustained loads in the force chains during impact (Fig. 8). Moreover, this observation is consistent with that reported by Muthuswamy and Tordesillas [27]. By examining the coordination number, it can be seen that rounded particles with less constraints collapse more easily, which helps to attenuate the boulder impact force.

2.6 Transmitted loads to rigid barrier

Figure 11 shows the computed time histories of the total transmitted loads (L) on the backside wall for four different particle shapes. The maximum total transmitted load (L) for angular particles occurs at 0.045 s, which occurs 0.010 s before rounded particles, suggesting that the time it takes to transmits load decrease with particle angularity. The same trend is supported by Fig. 8a, b, which also shows angular particles with smaller load diffusion angles. The smaller load diffusion angles enable a shorter load transmission distance. Moreover, the maximum total transmitted load for angular particles is 1.9 times larger compared to that of rounded particles.

Figure 12 shows a comparison of the maximum boulder impact force and the total transmitted load for simulations carried out for four different shapes. To minimise the effects of spatial variation of the initial packing arrangement of the particles on the impact dynamics, a total of 10 simulations were repeated at different impact locations of the cushioning layer for each particle shape. The spacing between each simulated impact differed by 50 mm in length. The dashed horizontal reference line is the estimated boulder impact force, without cushioning, using the following equation.

$$F = K_c 4000 v^{1.2} r^2 \quad (5)$$

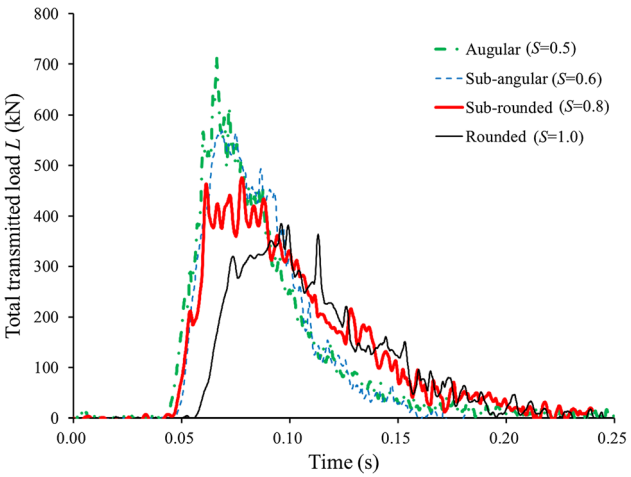

Fig. 11 Time histories of computed total transmitted loads with different particle shapes

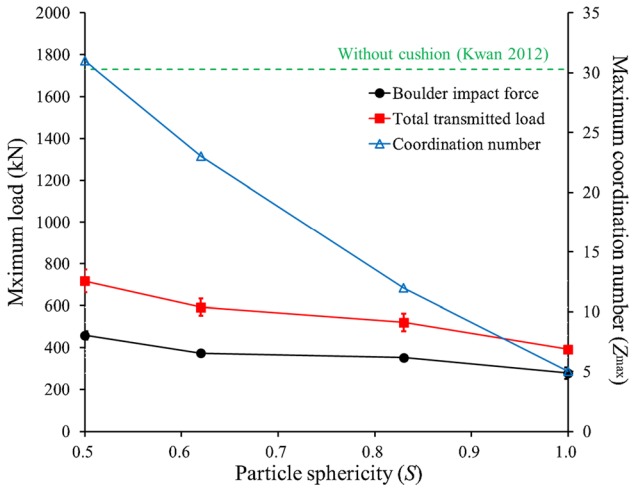

Fig. 12 Comparison of maximum boulder impact force and total transmitted load between different particle shapes

where F is the boulder impact force (N), K_c of 0.1 is recommended by Kwan [17] based on the case histories, v is the boulder velocity (m/s) and r is the boulder radius (m).

Compared with the estimated boulder impact force without cushioning, it can be found that at least 75% of the load is reduced when cushioning is considered. Furthermore, both the maximum boulder impact force (F_{max}) and maximum total transmitted load (L_{max}) decrease with increasing particle angularity. The average maximum boulder impact force and maximum total transmitted load for angular particles are about 1.8 times larger compared to that for rounded particles, respectively. The observed differences in the impact and transmitted loads are due to particle angularity. With increasing angularity, the forces chains also become more stable. Correspondingly, when possible, rounded rock fragments should be used for rock-filled gabions in the field to promote less stable force chains to enhance energy dissipation during impact.

Figure 13a, b shows a comparison of the computed maximum load distributions along the vertical and horizontal centrelines of the rigid barrier, respectively. In Fig. 13a, the horizontal axis shows the maximum transmitted load (L_{max}) and vertical axis shows the vertical depth (h/H) along the wall normalised by the barrier height. The transmitted loads are monitored from the backside wall (Fig. 9).

For all four shapes, small transmitted loads were observed at the top and bottom of the barrier at normalised heights of 0.04 and 0.96, suggesting that particle shape does not have an obvious effect on the vertical distribution of transmitted loads. For an assembly of rounded particles, the maximum transmitted load at the mid-height of wall is two to four times larger compared to that at a normalised height of 0.29 and 0.71, respectively. Furthermore, for sub-

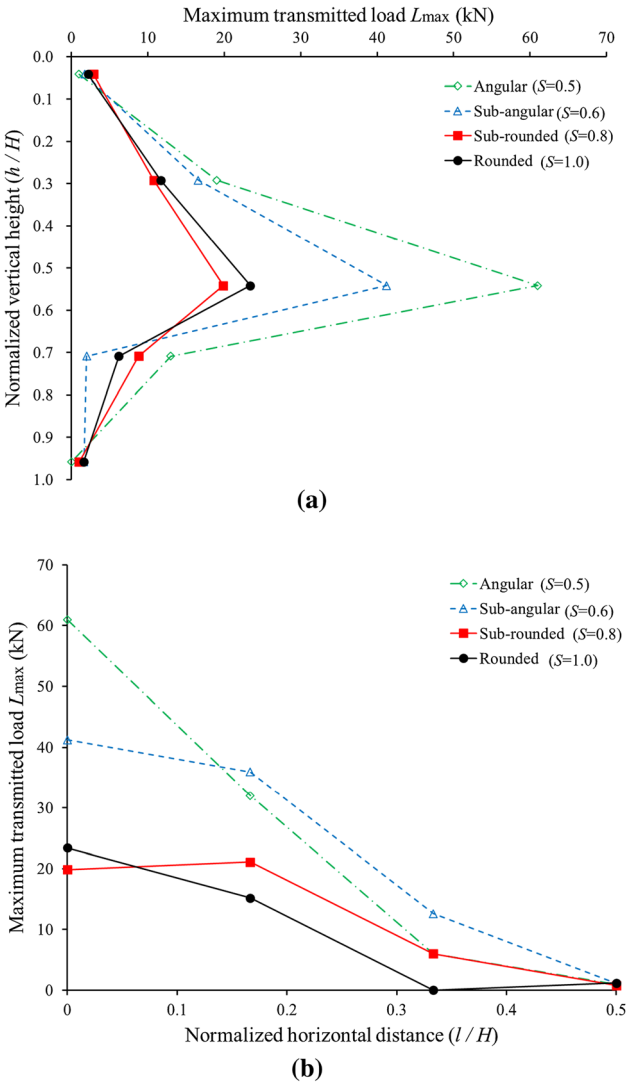

Fig. 13 Comparison of maximum transmitted loads among different particle shapes: **a** vertical distributions; **b** horizontal distributions

angular particles the maximum transmitted loads at the wall centre are about three and 21 times larger compared to that at a normalised height of 0.29 and 0.71, respectively. It is perhaps not surprising that transmitted loads are more concentrated at the centre of rigid barrier with increasing particle angularity because force chains are more stable (Fig. 9). The load diffusion angle decreases with the increasing particle angularity. Such an effect also contributes to load concentration at the centre of rigid barrier. The purpose of the cushioning materials is to reduce the concentrated loads on the rigid barrier. Therefore, this further supports that rounded particles should be adopted in field to ensure that the transmitted loads are distributed more uniformly.

Figure 13b shows the transmitted load distributions along the horizontal centreline of rigid barrier. For rounded particles, the maximum transmitted load at centre of wall is

1.5 times larger compared to that at the normalised horizontal distance of 0.17. This means the transmitted loads decrease with distance from the centre of backside wall. This is because more energy has dissipated over longer transmission distances [35]. Longer force chains generally consist of a larger number of particles, which collapse more easily [27]. Furthermore, for angular particles, the maximum transmitted load at the centre of wall is about two and 10 times larger compared to that at normalised horizontal distances of 0.17 and 0.33, respectively. To reduce the effects of load concentration, rounded rock fragments should be adopted in gabion baskets to ensure a more uniform load distribution.

3 Conclusions

A parametric study was conducted to investigate effects of particle shape on the cushioning performance of rock-filled gabions. Key findings from this study can be drawn as follows:

(a) Boulder penetration depth decreases with particle angularity. Assemblies of angular particles generally have a larger number of contacts, which lead to more stable force chains that can sustain higher loads. From the view point of rock-filled gabion cushioning design, perhaps a thicker cushioning layer may be adopted when rounded fragments are used in a gabion basket. A thickness of 1 m for an impact energy of 70 kJ was an appropriate thickness in this study.

(b) The maximum boulder impact force and total transmitted load increases by up to 180% with increasing particle angularity. This observation was directly attributed to more stable force chains. This observation further corroborates that rounded rock should be used where possible to reduce the load transmission to the structure under protection.

(c) Transmitted loads are more uniformly distributed along the cushioning layer as particle angularity decreases. The load diffusion angle of rounded particles is up to 20° larger compared to angular particles. If a more uniform cushioning effect is desired, rounded particles should be adopted.

Acknowledgements The authors are grateful for the financial support from the National Natural Science Foundation of China (51709052). The authors would like to gratefully acknowledge the support from the Fundamental Research Funds for the Central Universities (2019B07714). The authors are also grateful for financial support from the Research Grants Council of the Government of Hong Kong SAR, China (AoE/E-603/18; T22-603/15N; 16209717; 16212618; 16210219).

References

1. ASTRA (2008) Effects of rockfall on protection galleries. Federal Roads Office, Swiss
2. Altuhafi FN, Coop MR, Georgiannou VN (2016) Effect of particle shape on the mechanical behavior of natural sands. J Geotechn Geoenviron Eng 142(12):04016071
3. Bourrier F, Nicot F, Darve F (2008) Physical processes within a 2D granular layer during an impact. Granular Matter 10(6):415–437
4. Bhattacharya D, Kawamoto R, Karapiperis K (2020) Mechanical behaviour of granular media in flexible boundary plane strain conditions: experiment and level-set discrete element modelling. Acta Geotech. https://doi.org/10.1007/s11440-020-00996-8
5. Chen HX, Zhang LM, Zhang S (2014) Evolution of physical interactions in debris flow mixtures in the Wenchuan earthquake zone. Eng Geol 182:136–147
6. Choi CE, Goodwin G, Ng CWW, Cheung DKH, Kwan JSH, Pun WK (2016) Coarse granular flow interaction with slit-structures. Géotechn Lett 6(4):1–8
7. Chang CS, Deng Y, Meidani M (2018) A multi-variable equation for relationship between limiting void ratios of uniform sands and morphological characteristics of their particles. Eng Geol 237:21–31
8. Falagush O, McDowell GR, Yu H (2015) Discrete element modeling of cone penetration tests incorporating particle shape and crushing. Int J Geomech 15(6):1532–3641
9. Fu R, Hu X, Zhou B (2017) Discrete element modeling of crushable sands considering realistic particle shape effect. Comput Geotech 91:179–191
10. Geotechnical Engineering Office (1993) Guide to retaining wall design (Geoguide 1). Geotechnical Engineering Office, HKSAR
11. Hu X, Hu K, Tang J, You Y, Wu C (2019) Assessment of debris-flow potential dangers in the Jiuzhaigou Valley following the August 8, 2017, Jiuzhaigou earthquake, western China. Eng Geol 256:57–66
12. Hadda N, Wan R (2020) Micromechanical analysis of cyclic and asymptotic behaviors of a granular backfill. Acta Geotech 15:715–734
13. Iverson RM (1997) The physics of debris flows. Rev Geophys 35(3):245–296. https://doi.org/10.1029/97RG00426
14. Itasca (1999) PFC 3D-user manual. Itasca Consulting Group, Minneapolis
15. Janoo VC (1998) Quantification of shape, angularity, and surface texture of base course materials, special report 98-1 Cold Regions Research and Engineering Laboratory, US Army Corps of Engineers
16. Jesen RP, Edil TB, Bosscher PJ, Plesha ME, Kahla NB (2001) Effect of particle shape on interface behavior of DEM-simulated granular materials. Int J Geomech 1(1):1–19
17. Kwan JSH (2012) Supplementary technical guidance on design of rigid debris-resisting barriers. GEO Report No. 270, Geotechnical Engineering Office, HKSAR
18. Koo RCH, Kwan JSH, Lam C, Ng CWW, Yiu J, Choi CE, Ng AKL, Ho KKS, Pun WK (2016) Dynamic response of flexible rockfall barriers under different loading geometries. Landslides 14(3):905–916
19. Koo RCH, Kwan JSH, Lam C, Goodwin GR, Choi CE, Ng CWW, Yiu J, Ho KKS, Pun WK (2017) Back-analysis of geophysical flows using three-dimensional runout model. Can Geotech J 55(8):1081–1094
20. Lambert S (2007) Comportement mécanique de géocellules: application aux constituants de merlons pare-blocs cellulaires, PhD thesis, Université Joseph Fourier, Grenoble, France

21. Lambert S, Gotteland P, Nicot F (2009) Experimental study of the impact response of geocells as components of rockfall protection embankments. Nat Hazards Earth Syst Sci 9(2):459–467
22. Lambert S, Bourrier F (2013) Design of rockfall protection embankments: a review. Eng Geol 154:77–88
23. Lambert S, Heymann A, Gotteland P, Nicot F (2014) Real-scale investigation of the kinematic responses of a rockfall protection embankment. Nat Hazards Earth Syst Sci 14(5):1269–1281
24. Lee S, Winter MG (2019) The effects of debris flow in the Republic of Korea and some issues for successful risk reduction. Eng Geol 251:172–189
25. Lu X, Yao A, Su A, Ren X, Liu Q, Dong S (2019) Re-recognizing the impact of particle shape on physical and mechanical properties of sandy soils: a numerical study. Eng Geol 253:36–46
26. Mindlin RD, Deresiewicz H (1953) Elastic spheres in contact under varying oblique forces. J Appl Mech 20:327–344
27. Muthuswamy M, Tordesillas A (2006) How do interparticle contact friction, packing density and degree of polydispersity affect force propagation in particulate assemblies? J Stat Mech Theory Exp 2006:P09003
28. Ng CWW, Choi CE, Law RPH (2013) Longitudinal spreading of granular flow in trapezoidal channels. Geomorphology 194:84–93
29. Ng CWW, Choi CE, Su AY, Kwan JSH, Lam C (2016) Large-scale successive impacts on a rigid barrier shielded by gabions. Can Geotech J 53(10):1688–1699
30. Ng CWW, Choi CE, Liu* LHD, Wang Y, Song D, Yang N (2017) Influence of particle size on the mechanism of dry granular run-up on a rigid barrier. Géotechn Lett 7(1):79–89
31. Ng CWW, Choi CE, Koo RCH, Goodwin GR, Song D, Kwan JSH (2018) Dry granular flow interaction with dual-barrier systems. Géotechnique 68(5):386–399
32. Shin H, Santamatina JC (2013) Role of particle angularity on the mechanical behavior of granular mixtures. J Geotechn Geoenviron Eng 139(2):353–355
33. Suh HS, Kim KY, Lee J, Yun TS (2017) Quantification of bulk form and angularity of particle with correlation of shear strength and packing density in sands. Eng Geol 220:256–265
34. Shen W, Zhao T, Zhao J, Dai F, Zhou GGD (2018) Quantifying the impact of dry debris flow against a rigid barrier by DEM analyses. Eng Geol 241:86–96
35. Su Y, Cui Y, Ng CWW, Choi CE, Kwan JSH (2019) Effects of particle size and cushion thickness on the impact performance of gabions. Can Geotech J 56(2):198–207
36. Su Y, Choi CE, Ng CWW, Lam C, Kwan JSH, Wu G, Huang J, Zhang Z (2019) Eco-friendly recycled crushed glass for cushioning boulder impacts. Can Geotech J 56(9):1251–1260
37. Shi L, Zhao W, Sun B, Sun W (2020) Determination of the coefficient of rolling friction of irregularly shaped maize particles by using discrete element method. Int J Agric Biol Eng 13(2):15–25
38. Thornton C (2000) Numerical simulations of deviatoric shear deformation of granular media. Geotechnique 50(1):43–53
39. Tordesillas A, Steer CAH, Walker DM (2014) Force chain and contact cycle evolution in a dense granular material under shallow penetration. Nonlinear Process Geophys 21(2):505–519
40. Takahashi T, Nakagawa H (1991) Prediction of stony debris flow induced by severe rainfall. J Jpn Soc Erosion Control Eng 44(3):12–19 **(In Japanese)**
41. Takahashi T (2014) Debris flow: mechanics, prediction and countermeasures. CRC Press, London
42. Unland G, Al-Khasawneh Y (2009) The influence of particle shape on parameters of impact crushing. Miner Eng 22(2009):220–228
43. Ueda T, Matsushima T, Yamada Y (2013) DEM simulation on the one-dimensional compression behaviour of various shaped crushable granular materials. Granular Matter 15(5):675–684
44. Utili S, Zhao T, Houlsby GT (2015) 3D DEM investigation of granular column collapse: evaluation of debris motion and its destructive power. Eng Geol 186:3–16
45. Valagussa A, Frattini P, Crosta GB (2014) Earthquake-induced rockfall hazard zoning. Eng Geol 182:213–225
46. Wadell H (1932) Volume, shape and roundness of rock particles. J Geol 40:443–451
47. Wnsrich CM, Katterfeld A (2012) Rolling friction as a technique for modelling particle shape in DEM. Powder Technol 217(2012):409–417
48. Wang Y, Song E (2019) Discrete element analysis of the particle shape effect on packing density and strength of rockfills. Rock Soil Mech 40(6):2416–2426
49. Xiao Y, Long L, Evans TM, Zhou H, Liu H, Stuedlein AW (2019) Effect of particle shape on stress-dilatancy responses of medium-dense sands. J Geotech Geoenviron Eng 145(2):04018105
50. Xiao Y, Stuedlein AW, Ran JY, Evans TM, Cheng L, Liu HL, van Paassen LA, Chu J (2019) Effect of particle shape on strength and stiffness of biocemented glass beads. J Geotech Geoenviron Eng 145(11):06019016
51. Xu W, Liu G, Yang H (2020) Study on the mechanical behavior of sands using 3D discrete element method with realistic particle models. Acta Geotech
52. Yang J, Wei LM (2012) Collapse of loose sand with the addition of fines: the role of particle shape. Geotechnique 62(12):1111–1125
53. Yang J, Luo XD (2015) Exploring the relationship between critical state and particle shape for granular materials. J Mech Phys Solids 84:196–213
54. Yang J, Luo XD (2017) The critical state friction angle of granular materials: does it depend on grading? Acta Geotech 12(6):1–13
55. Zhang S, Hungr O, Slaymaker O (1996) The calculation of impact force of boulders in debris flow. In: Du R (ed) Debris flow observation and research. Science Press, pp 67–72
56. Zhou W, Ma G, Chang X, Zhou C (2013) Influence of particle shape on behavior of rockfill using a three-dimensional deformable DEM. J Eng Mech 139(12):1868–1873
57. Zhang L, Lambert S, Nicot F (2017) Discrete dynamic modelling of the mechanical behaviour of a granular soil. Int J Impact Eng 103:76–89
58. Zhou W, Yang L, Ma G, Xu K, Lai Z, Chang X (2017) DEM modelling of shear bands in crushable and irregularly shaped granular materials. Granular Matter 19(2):1–12
59. Zhang S, Zhang L, Li X, Xu Q (2018) Physical vulnerability models for assessing building damage by debris flows. Eng Geol 247:145–158
60. Zheng J, He H, Alimohammadi H (2020) Three-dimensional Wadell roundness for particle angularity characterization of granular soils. Acta Geotech. https://doi.org/10.1007/s11440-020-01004-9